

---

**APST**

---

**Asia-Pacific Journal of Science and Technology**<https://www.tci-thaijo.org/index.php/APST/index>Published by the Research and Technology Transfer Affairs Division,  
Khon Kaen University, Thailand

---

**Application of aluminum and black rubber heat absorber for solar-base distillation with double slanted-glassed configuration**Nattadon Pannucharoenwong<sup>1,\*</sup>, Phadungsak Rattanadecho<sup>1</sup>, Victoria Timchenko<sup>2</sup>, Snunkhaem Echaroj<sup>1</sup> and Kriengkrai Nabudda<sup>3</sup><sup>1</sup> Department of Mechanical Engineering, Thammasat University, Pathumthani, Thailand<sup>2</sup> School of Mechanical and Manufacturing Engineering, the University of New South Wales, Sydney, Australia<sup>3</sup> Department of Mechanical Engineering, Khon Kaen University, Khon Kaen, Thailand

\*Correspondent author: pnattado@engr.tu.ac.th

Received 11 March 2019

Revised 12 July 2019

Accepted 22 July 2019

---

**Abstract**

The aim of this research is to generate a mathematical model and investigate the efficiency of aluminum and black rubber as heat absorber for the Solar-based Double one-Direction slanted-Glass distillation unit (SDDG) by varying the size of the heat absorber. The heat absorber was placed inside the secondary liquid layer of the distillation station. Experiments were conducted by varying the heat absorber plate from 10% to 90% of the second layer's area. The volume of distilled water was monitored to calculate the efficiency of the distillation unit. Results showed the highest distilled volume of 1.60 litre per day was obtained when the size of aluminum heat absorber was 10%, which produced an average efficiency of 26.34%. Furthermore, a reduction in the distilled volume and efficiency to 0.98 litre per day and 17.3% was observed when the aluminum heat absorber size was increased to 90%. The same trend can be observed for SDDG with black rubber as a heat absorber. However, the efficiency of equivalent size of black rubber is significantly smaller than aluminum due to lower thermal conductivity and material shrinkage when exposed to the solar radiation. The maximum productivity achievable for SDDG with black rubber heat absorber was only 1.17 litre per day. This indicated better heat transfer for smaller heat absorber. The reason is because it is harder for light to pass through the heat absorber with larger area causing the efficiency to drop dramatically as area of heat absorber increased. Polynomial equations were successfully proposed for prediction of productivity from operating time and efficiency from the size of heat absorber.

**Keywords:** Distillation unit, Heat transfer, Heat absorber, Solar radiation

---

**1. Introduction**

Water distillation by using solar-based system is among the environmental friendly and low maintenance alternative method for effective water treatment. It is also sustainable because it harnesses energy from unlimited source of sunlight. The distillation system was employed along with reverse osmosis technology to effectively treat waste water with high biological oxygen demand (BOD) content [1]. The shape and size of heat absorber system had a significant effect on the solar adsorption area. An origami structured heat receiver was proposed to improve heat adsorption and reduce undesirable loss through heat reflection phenomena [2-3].

Many different type of solar-based distillation methods were investigated over the years including, Humidification-Dehumidification (HD), Indirect Desalination (ID) and Basin Distillation (BD). The HD method employed dry air as a working fluid, which initially receive moisture from the evaporated salted concentrated liquid employed as heat transfer medium. Consequently, vaporization of salted concentrated liquid resulted in an increase in humidity of the dry air. Then it is moved along with pure water vapour to be condensed and collected as drinkable water [4-5]. In contrast, ID method consisted of a solar collector, heat fluid and heat exchangers [6]. BD is among the simple type of process employing heat transfer from sunlight through the glass covered channel

and absorbed by the heating fluid [7]. However, compared with other type of distillation system BD produce relatively low yield of clean water and it is also inexpensive. More research need to be conducted to get rid of these disadvantages for the BD system. Marugravel et. al. reported an increase in clean water yield when double layer system was used instead of the common vertical BD system [8]. Among many different methods to improve the efficiency of BD, an increase in heating fluid outlet per area was found to be effective. Addition of fins along the condenser wall of the distillation unit resulted in an increase in system efficiency of approximately 11% to 14% [9]. A novel underground solar-based distillation unit capable of producing 3 kg of distilled water per  $\text{m}^3$  of solar collector was reported [10].

Many researches utilized nanoparticle to increase water and thermal efficiency of the water distillation system. Qin et al. investigated an increase in thermal efficiency by 4.8% and 6.7% when silver and gold nanoparticles were added to the operating fluid inside the distillation unit [11]. Titanium nitrate was also employed as nanoparticle along with membrane technology to enhance thermal efficiency and heat flux of the solar-base distillation unit [12-13]. These nanoparticles were found to increase thermal conductivity of the heat adsorbed medium which results in a remarkable increase in distilled water yield [14]. Another highly efficient material used as heat absorber was 2-dimensional defective tungsten oxide [15]. Hong et al. reported an almost full-spectrum absorption of solar light on Cu nanodot-embdded N-doped graphene urchins with high accessibility and capable of self-float on water [16]. Although these techniques can improve the thermal efficiency of the distillation system but they are expensive and can pose health problems, such as respiratory problems and Alzheimer.

The purpose of this research is to observe how the Solar-based Double slanted-Glass Distillation system (SDDG) operates using two different type of heat absorbers; the aluminum and black rubber. Additionally, the size of heat absorber were vary from 10 to 90% of the secondary layer area in order to investigate how the size effect the distillation system. Aluminium and black rubber were chosen for this research because these two materials have adequate thermal conductivity and are easy to manufacture. The evaluated parameters included solar flux, temperature at different location inside the SDDG, and productivity of both upper level and bottom level. An engineering Equation Solver (EES) software was employed to solve for the efficiency of the distillation unit. Mathematical models were developed to simulate the water productivity from operating time and efficiency from the size of the heat absorber.

## 2. Materials and methods

### 2.1 Experimental setup

This research studied the double-glass layer previously developed by another group of researcher. The area of the base foundation of the distillation unit was 150 cm x 100 cm and 20 cm high as shown in Figure 1. Each channel of the distillation still contained an inlet and outlet port. The bottom section of the distillation unit contained layer of aluminum heat absorber, insulator and wooden floor. The slanted-glass makes an angle of 14 o with the floor. Multiple steps were created inside the top layer of the distillation unit to increase effective area for heat adsorption activities.

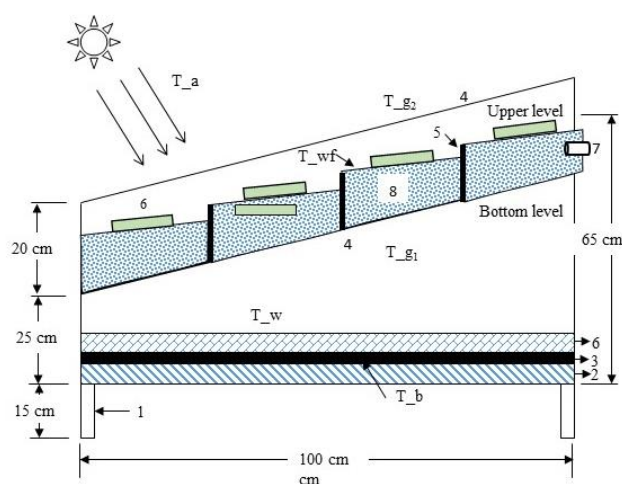


**Figure 1** Experimental setup for the double slanted-glass distillation unit: 1. Stand for the distillation unit, 2. Compressed wood partition, 3. Insulator, 4. Glass cover, 5. Glass partition for each steps in the upper level, 6. heat absorber, 7. Inlet water and 8. Water. ( $T_b$  is temperature of the insulator,  $T_w$  is the temperature of water in the bottom level,  $T_{wf}$  is temperature of water in the upper level,  $T_{g1}$  is glass cover for the bottom level,  $T_{g2}$  is glass cover for the upper level, and  $T_a$  is temperature of the atmosphere).

Light intensity and accumulated distilled water was monitored and used to calculate the efficiency of the distillation unit. Individual records were kept for distillation unit with different size of the aluminum heat absorber. The temperature at five different location inside the distillation unit was measured by J-type thermocouple which are attached to the digital meter for continuous data logging ( $T_b$ ,  $T_w$ ,  $T_{gl}$ ,  $T_{wf}$  and  $T_{g2}$ ). Approximately 0.075 L of water is poured into the bottom still container and 0.024 L of water is poured into the upper still container at the top of the distillation unit. Relative humidity was calculated from wet bulb and dry bulb temperature. All data were collected every hour.

## 2.2 Heat transfer principles

Radiation from the sun penetrates the transparent glass cover at the top of the distillation unit. Heat created by radiation is absorbed by untreated water and the wall surfaces of the still container. Consequently, untreated water will gradually convert to water vapor due to an increase in vapor pressure beyond the equilibrium threshold point. Water vapor will flow up to the upper glass wall and condensed back into liquid form which will roll along the slanted glass wall by gravity into a gutter that is separated from the still. The glass wall is designed to be slanted to prevent condensed water from falling back into the still container. The gutter is also designed to slant slightly to carry treated water to the secondary still container at the bottom of the distillation unit.

## 2.3 Calculation for heat transfer through radiation

Solar radiation per hour ( $I$ ) is calculated by multiplying the solar radiation measured per day with the ratio of accumulated solar radiation per hour to accumulated solar radiation per day.

$$I = Hr_i \quad (1)$$

$$r_i = \frac{\pi}{24} (a + b \cos \omega) \frac{\cos \omega - \cos \omega_s}{\sin \omega_s - \left(\frac{2\pi\omega_s}{360}\right) \cos \omega_s} \quad (2)$$

Where  $a = a_1 + a_2 \sin(\omega_s - 60)$ ,  $b = b_1 + b_2 \sin(\omega_s - 60)$  and  $\omega_s$  represent the sunset hour angle which is the incidence angle that occur when the solar radiation strikes the specific area. The values of  $a_1$ ,  $a_2$ ,  $b_1$ , and  $b_2$  depend solely on the location of distillation setup in Thailand. For this study the distillation unit was established at the Ubonratchathani station where the coefficients are:  $a_1 = 0.76$ ,  $a_2 = -0.031$ ,  $b_1 = 0.207$  and  $b_2 = 0.238$  (17).

Heat that impacts on the object is in the form of energy that includes radiation from all direction. Part of the energy is reflected, adsorbed and travel through the object. These phenomenon are referred to as  $\rho$  is reflectivity,  $\alpha$  is absorptivity and  $\tau$  is transmissivity.

## 2.4 Heat transmission inside solar-based distillation unit

A major portion of the transmissivity heat along the solar-based distillation is lost from the system. This results in a reduction in the rate of water distillation process, because only a small portion of heat is delivered to the water the upper still container. Heat is lost through this route is because part of the radiation is reflected from the protective cover of the solar-based distillation. Heat that is transmitted will pass through the protective cover and accumulates in body of water. Heat transfer sequence for solar-based distillation unit are as follows:

1. Solar radiation that is absorbed by the protective cover ( $Q_{S.AG}$ )
2. Solar radiation that is transmitted through the protective cover ( $Q_{TR}$ )
3. Solar radiation that is absorbed by water inside the still container ( $Q_{S.AW}$ )
4. Heat transfer from the protective cover to the atmosphere in radiation mode ( $Q_{RO}$ )
5. Heat transfer from the protective cover to the atmosphere in convection mode ( $Q_{CO}$ )
6. Heat transfer from surface of water to the protective cover in radiation mode ( $Q_{RI}$ )
7. Heat transfer from surface of water to the protective cover in convection mode ( $Q_{CI}$ )
8. Heat loss from the top and bottom of the distillation unit ( $Q_L$ )
9. Heat transfer from water vapor to the protective cover ( $Q_E$ )
10. Heat loss from the condensed water ( $Q_{distill}$ )

Energy balance at different locations inside the solar-based distillation unit are shown in equation 3 to 8.

- a. Energy balance for the insulator

$$m_b C_{pb} \frac{dT_b}{dt} = I(t)A_b - q_{cbw} - q_{loss} \quad (3)$$

- b. Energy balance for water in the upper still container (level 1)

$$m_w C_{pw} \frac{dT_w}{dt} = I(t)A_w + q_{cbw} - q_{rwg1} - q_{cwg1} - q_{ewg1} \quad (4)$$

- c. Energy balance for glass surface (level 1)

$$m_g C_{pg} \frac{dT_{g1}}{dt} = I(t)A_{g1} + q_{rwg1} + q_{cwg1} + q_{ewg1} - q_{cg1wf} \quad (5)$$

- a. Energy balance for water in the bottom still container (level 2)

$$m_{wf} C_{pw} \frac{dT_{wf}}{dt} = I(t)A_{wf} + q_{cg1wf} - q_{cwf2} - q_{rwf2} - q_{ewf2} + q_{absorber} \quad (6)$$

- d. Energy balance for glass surface (level 2)

$$m_g C_{pg} \frac{dT_{g2}}{dt} = I(t)A_{g2} + q_{cwf2} + q_{rwf2} + q_{ewf2} - q_{rg2,sky} - q_{cg2,a} \quad (7)$$

- b. Condensation for the two levels inside distillation unit

$$\frac{dm_c}{dt} = h_{ewg1} \frac{(T_w - T_{g1})}{h_{fg @ T_w}} + h_{ewf2} \frac{(T_{wf} - T_{g2})}{h_{fg @ T_{wf}}} \quad (8)$$

In these equations,  $T_b$  is bottom insulation temperature,  $T_w$  is bottom water surface,  $T_{g1}$  is bottom glass surface,  $T_{wf}$  upper water surface, and  $T_{g2}$  is the upper glass surface. It is assumed that the room temperature is 25 °C. The bottom insulator mass, bottom water mass, glass mass, and upper water mass are represented by variables including  $m_b$ ,  $m_w$ ,  $m_g$  and  $m_{wf}$ . The value of each variable and constants are shown in Table 1.

### 2.5 Heat absorption by object inside the distillation unit

The general equation employed to find heat that is absorbed by a specific material is as follows:

$$q_{absorber} = \alpha (I_b \tau_{wb} + I_a \tau_{wd}) \quad (9)$$

Where  $\alpha$  represents the adsorption radiation coefficient of the specific material,  $I_b$  represented the amount of solar radiation per hour,  $\tau_{wb}$  is solar radiation transferred to the atmosphere due to absorption of steam,  $\tau_{wd}$  is solar radiation transferred to the atmosphere by mean of scattering.

**Table 1** Parameters for operating the double slanted-glass distillation unit [18].

Operating conditions	Value	Unit
Mass of glass ( $m_g$ )	6	kg
Mass of bottom insulator ( $m_b$ )	10	kg
Glass specific heat ( $C_{pg}$ )	800	J/(kg °C)
Water specific heat ( $C_{pw}$ )	4,178	J/(kg °C)
Glass emissivity ( $\varepsilon_g$ )	0.88	-
Water emissivity ( $\varepsilon_w$ )	0.96	-
Radiation absorption of glass ( $\alpha_g$ )	0.0475	-
Radiation absorption of water ( $\alpha_w$ )	0.05	-
Reflectivity of glass ( $\rho_g$ )	0.0735	kg/cm <sup>3</sup>
Overall heat transfer coefficient ( $U_b$ )	14,	W/(m <sup>2</sup> K)
$h_{bw}$	135	W/(m <sup>2</sup> K)
$h_{cg1wf}$	25	W/(m <sup>2</sup> K)

## 2.6 Efficiency of Solar Still Water Refiner Calculation

The general equation employed to find the efficiency ( $\eta$ ) of heat transfer inside the distillation unit is as follows:

$$\eta = \frac{\sum \dot{m}_c h_{fg}}{\sum I} \quad (10)$$

Where  $\dot{m}_c$  represents the condensation ratio,  $h_{fg}$  represent latent heat and I represent solar radiation condensation.

## 2.7 Equation solving methods

Engineering Equation Solver (EES) computer based program was employed to solve for the efficiency of solar radiation inside the double slanted-glass distillation unit. Variables for condensation were solved through solar function (equation 3 to 8) for  $T_b$ ,  $T_w$ ,  $T_{g1}$ ,  $T_{wf}$  and  $T_{g2}$ . The obtained value of latent heat ( $h_{fg}$ ) for both upper and bottom level are used to find condensation ratio and then the efficiency of the distillation unit as shown in equation 10. The EES process followed a logical route as shown in Figure 2.

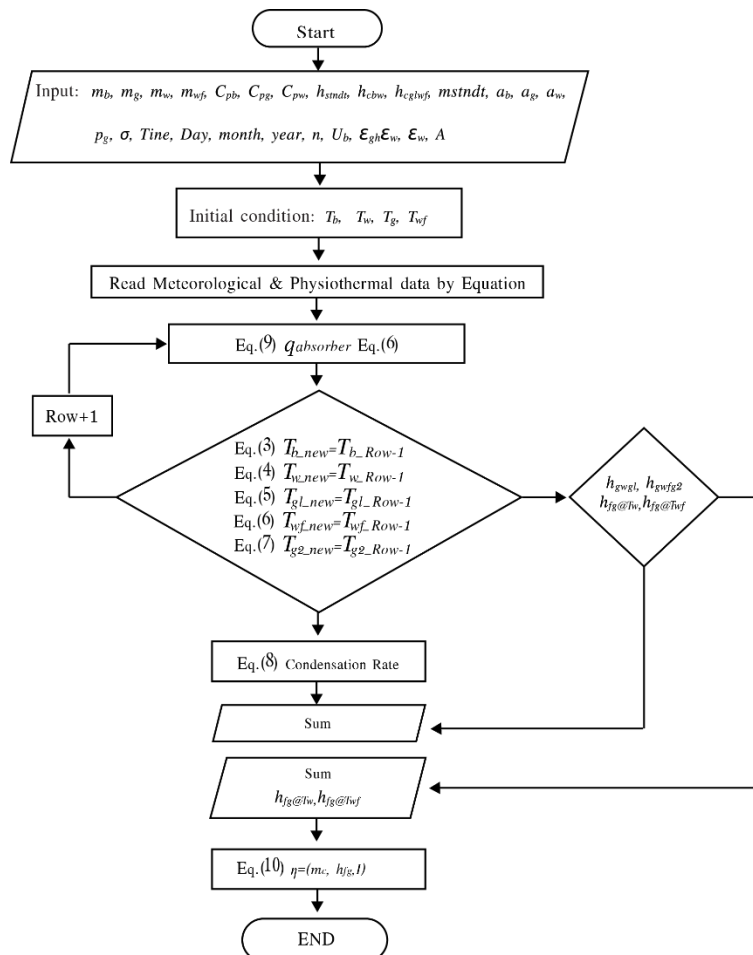


**Figure 2** Logical path integrated in the EES technique for solving temperature at each location and efficiency of each type of heat absorber.

### 3. Results and discussion

#### 3.1 Condensation from solar radiation

In this experiment, aluminum absorbers with size from 10 to 90 % of the bottom water surface area were examined and evaluated based on the temperature variable, amount of condensed water and efficiency of the distillation unit. Figure 3 demonstrated the flow of solar flux in one day using 10% aluminum absorber sheet. It was found that the average solar flux during condensation was  $393.80 \text{ W/m}^2$  and reached a maximum of  $708.33 \text{ W/m}^2$  at 13:00 P.M for aluminum heat absorber. The solar radiation for black rubber is slightly higher due to the different placement of the distillation unit containing black rubber heat absorber. The difference in solar flux is especially noticeable at the peak hour. The total solar flux at this location is similar to results obtained in Chennai, India [1].

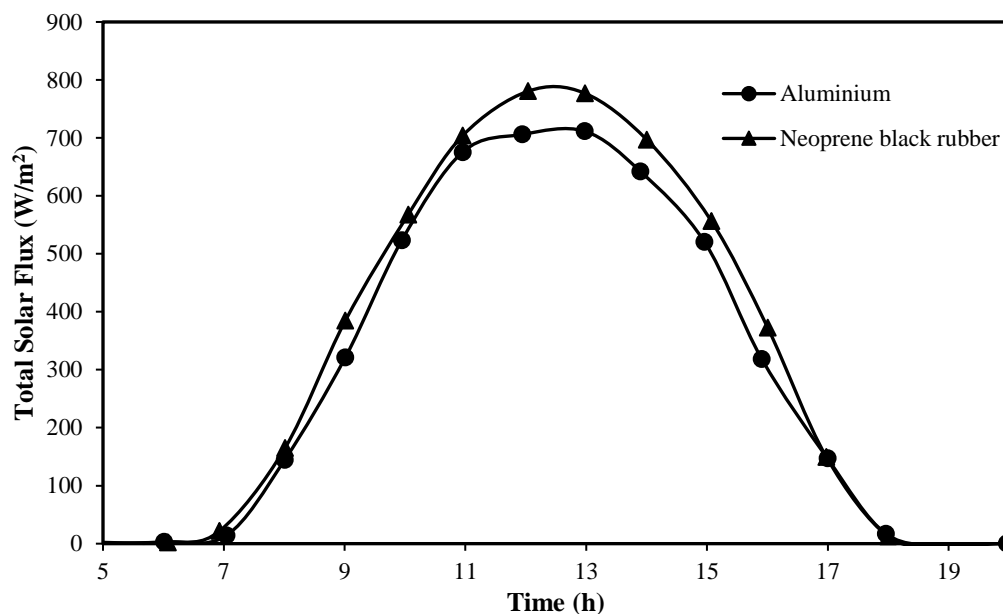


**Figure 3** Monitoring solar flux from 7:00 A.M. to 19:00 P.M. Aluminum and Black rubber heat absorber size 10%.

#### 3.2 Temperature of water and glass surfaces

Figure 4 illustrates the calculated temperature from different location inside the solar-based distillation unit at different time during the operation. The difference between the upper glass surface and upper water surface was higher compared with the difference between the bottom glass surface and bottom water surface. The highest temperature of  $47.2^\circ\text{C}$  was found between water and glass surface in both levels around 15 hours after the start of distillation (15:00 P.M.). The difference of temperature between water and glass surface for the upper level and bottom level was  $1.67^\circ\text{C}$  and  $1.37^\circ\text{C}$ . This observation indicated that the upper level had more condensation activity compared with the bottom level. Temperature inside the black rubber followed the same trend. However, the maximum temperature achievable for black rubber is higher than that of aluminum heat absorber as shown in Figure 4 (B). The temperature gap between first and second layer of glass is smaller when black rubber is used as heat absorber due to inefficient heat transfer potential. A comparison between the temperature inside SDDG with aluminum and black rubber are shown in Figure 4 (C). The maximum temperature achievable is relatively high even when there is no addition of phase change materials [19].

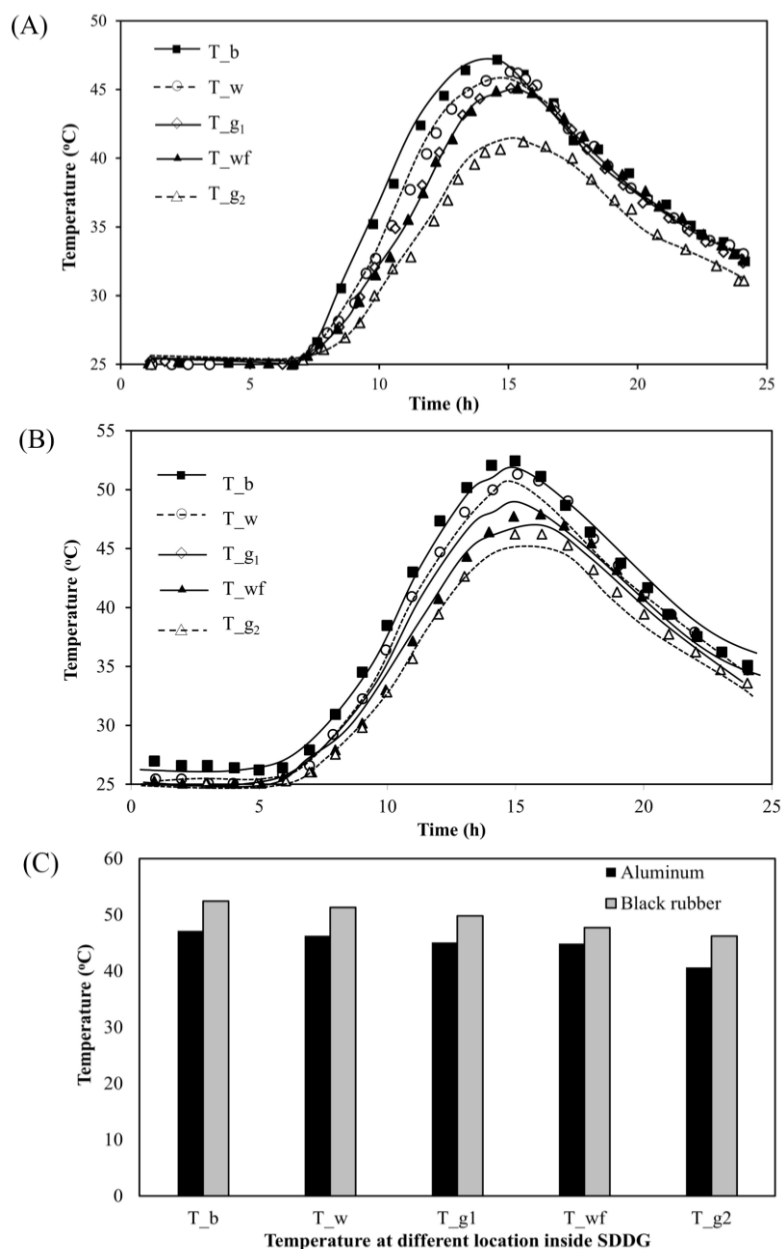


**Figure 4** Temperature measured at different location inside the SDDG containing (A) aluminum, (B) black rubber heat absorbers and (C) comparison between the two material 15 hours after the start of operation.

### 3.3 Accumulated water condensation ratio

Figure 5 demonstrated the accumulated water productivity from the first layer (upper level) and the second layer (bottom level). The accumulated water condensation rate in the upper level and bottom level of SDDG with aluminum heat absorber was  $0.51 \text{ l/m}^2$  and  $0.92 \text{ l/m}^2$ , respectively. However the condensation rate for the upper and bottom level of the SDDG with black rubber heat absorber were  $0.57 \text{ l/m}^2$  and accumulative refined water was  $0.95 \text{ l/m}^2$ . The bottom level of SDDG with black rubber gave higher condensation rate due to the shrinkage of black rubber material which resulted from the solar penetration into the bottom level of the distillation unit. It can be observed that condensation does not take place during the first 3 hours of operation. This is because the solar heat input is use evaporation as latent heat first before being utilized for raising the temperature. It can be observed that the total productivity from distillation unit with aluminum heat absorber is relatively higher compared with black rubber heat absorber. The total distilled water productivity from aluminum and black rubber were approximately 1.60 and 1.17 liter when the area of heat absorber was equaled to 10% of the bottom layer.

The generation of distilled water SDDG at different times was modeled by using polynomial equation as shown in equation 11 (aluminum) and 12 (black rubber). 6<sup>th</sup> order polynomial was employed to predict the efficiency of the distillation unit since the coefficients in both equations resulted in a predictions that were very close to the experimental data where  $R^2$  very close to 1.

$$\text{Productivity (liter)} = 4x10 - 7t6 - 3x10 - 5t5 + 0.0008t4 - 0.0096t3 + 0.0528t2 - 0.1245t + 0.1111 \quad (11)$$

$$R^2 = 0.9997$$

$$\text{Productivity (liter)} = 4E - 07t6 - 3E - 05t5 + 0.0007t4 - 0.0076t3 + 0.0379t2 - 0.0778t + 0.05 \quad (12)$$

$$R^2 = 0.9994$$

In equation 11 and 12, t represents the operating time for the distillation unit

According to Figure 6 an increase in size of both type of heat absorber resulted in a reduction in efficiency of the distillation unit. An incremental increase in aluminum heat absorber size by 10% resulted in approximately a reduction in efficiency by 2 to 5%. However, the average efficiency of the distillation unit is approximately 26%. The efficiency of black rubber is significantly lower than that of aluminum heat absorber.

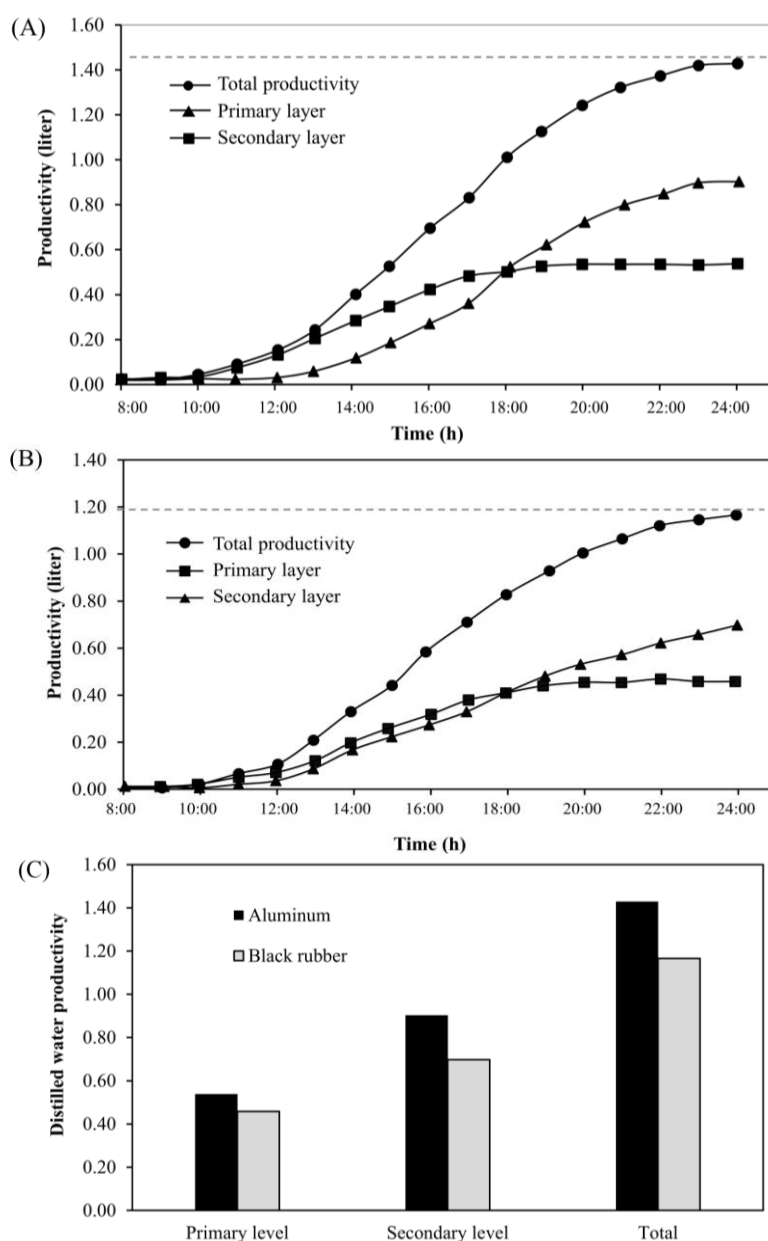


**Figure 5** Productivity of water condensation using (A) aluminum, (B) black rubber heat absorber 10% size and (C) productivity of distilled water after 24 hours of operation.



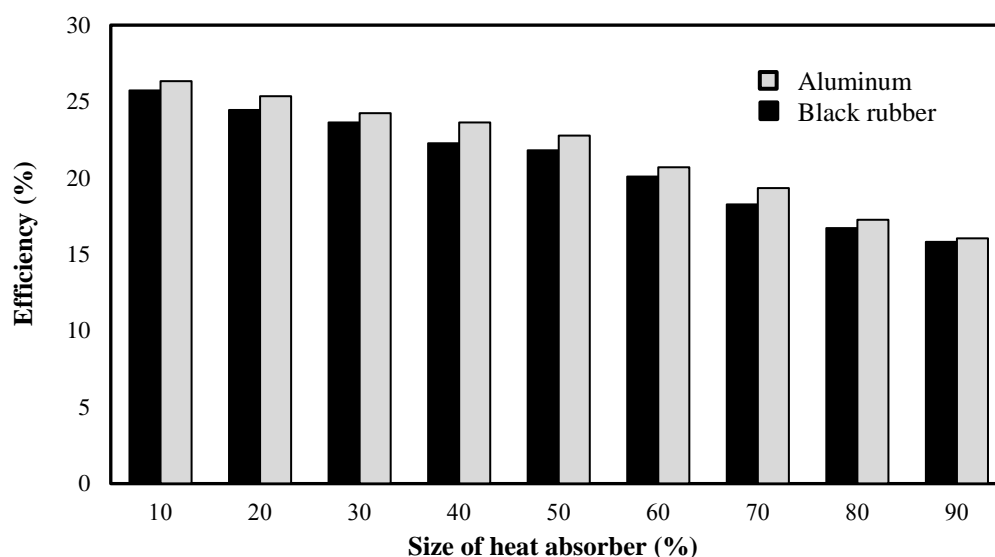


**Figure 6** Efficiency of the double slanted-glass distillation unit.

Data collected were tabulated for different size of aluminum heat absorber from 10 to 90% of the water surface area. Solar intensity is considered as an important parameter that influence the efficiency and productivity of the unit [20]. As shown in Table 2, an increase in the size of aluminum heat absorber resulted in a decrease in efficiency. The efficiency peaked when the heat absorber size was 10% (25.99%) and the lowest efficiency was realized when the heat absorber size was 90% (15.02%). It is obvious that the efficiency of aluminum heat absorber is higher than that of black rubber. This is due to the higher thermal conductivity of aluminum heat absorber compared with that of black rubber [21]. Black rubber also suffered from efficiency reduction due to material shrinkage when exposed to heat [22]. The amount of distilled water produced per day from 10% aluminum heat absorber is relatively higher compared with hybrid solar distillation unit [23]. However the solar intensity of the distillation unit developed in this experiment ( $820 \text{ W/m}^2$ ) is significantly lower than that of the solar chimney type distillation unit ( $982 \text{ W/m}^2$ ) and that of a tubular still for desalination ( $1000 \text{ W/m}^2$ ) [24]. This is due to the effective air circulation inside the solar chimney type distillation unit which promote efficient heat transfer process [25]. A comparison of solar intensity between this work and the other works are illustrated in Figure 7. The lower solar intensity collected by SDDG designed in this work compared with the other two researches is due to the size of the SDDG which is significantly smaller than both Chimney-type and Tubular-Type distillation unit. Additionally, the installation location is also an important consideration which influence the outcome of solar intensity as shown in Figure 7.

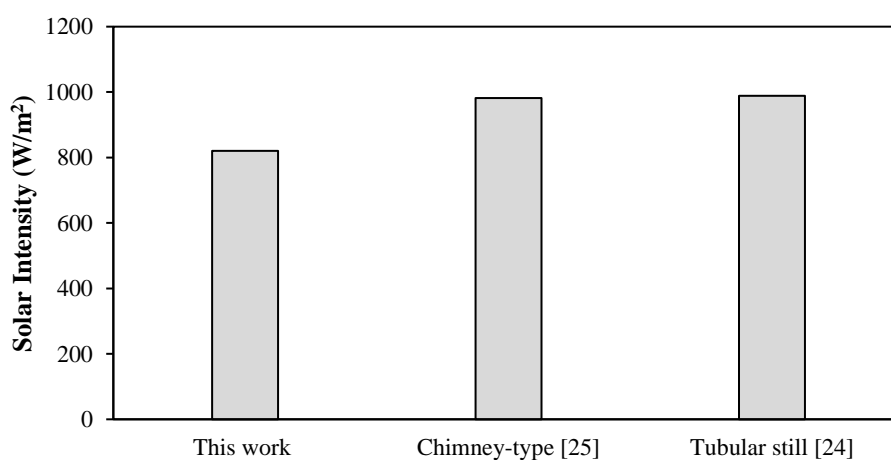


**Figure 7** Comparison of solar intensity of SDDG with a chimney and tubular still.

Mathematical modeling of the distillation unit's efficiency as a function of the size of heat absorber was performed for both aluminum and black rubber material. Polynomial equation was found give the most accurate efficiency with  $R^2$  close to 1. Equation 13 (aluminum) and equation 14 (black rubber) demonstrated the polynomial equation obtained from the modeling process.

$$\text{Efficiency (\%)} = -0.0005x^6 + 0.0178x^5 - 0.2175x^4 + 1.2487x^3 - 3.4599x^2 + 3.2071x + 24.919 \quad (13)$$

$$R^2 = 0.9979$$

$$\text{Efficiency (\%)} = -0.0007x^6 + 0.0203x^5 - 0.2364x^4 + 1.2942x^3 - 3.4328x^2 + 3.1544x + 25.537 \quad (14)$$

$$R^2 = 0.9978$$

Where x represents the size of heat absorber in percentage

**Table 2** Average solar intensity, the amount of distilled water and efficiency for different aluminum heat absorber.

No.	Heat absorber size (%)	Average solar intensity		Amount of distilled water per day (8 h)		Efficiency	
		Al. <sup>1</sup>	BR. <sup>2</sup>	Al. <sup>1</sup>	BR. <sup>2</sup>	Al. <sup>1</sup>	BR. <sup>2</sup>
		(W/m <sup>2</sup> )	(W/m <sup>2</sup> )	(litre)	(litre)	(%)	(%)
1	10%	393.80	487.36	1.60	1.17	26.34	25.72
2	20%	395.39	493.91	1.44	1.16	24.94	24.29
3	30%	393.87	466.20	1.42	1.14	24.36	23.55
4	40%	390.53	466.67	1.37	1.11	24.07	22.27
5	50%	377.89	441.67	1.32	1.05	23.24	21.91
6	60%	391.94	458.33	1.19	1.03	21.59	20.21
7	70%	404.10	473.93	1.13	0.97	20.22	18.14
8	80%	432.22	461.11	1.08	0.94	18.73	16.71
9	90%	438.03	463.89	0.98	0.90	17.29	15.76

Note: <sup>1</sup> Aluminum and <sup>2</sup> Black rubber

#### 4. Conclusions

Experimental outcome demonstrated the effectiveness of aluminium as a heat absorber for the double slanted-glass distillation unit. An increase in the area of the aluminium heat absorber was found to reduce the efficiency of the distillation unit. This resulted in a reduction in the amount of water condensed from the unit. When 10% aluminium heat absorber was used the highest amount of condensed water was 1.60 litre per day and the accumulative efficiency was 26.34%. In contrary, 90% aluminium heat absorber provided the lowest efficiency with productivity of 0.98 litre of condensed water per day and an accumulative efficiency of 17.29%. The efficiency of the black rubber heat absorber is smaller compared with aluminum heat absorber at all sizes. The difference between glass surface and water surface for the upper level and bottom level of SDDG with aluminum exchanger was 1.67 °C and 1.37 °C, which provide sufficiency heat transfer for an effective usage of sunlight for water condensation. For black rubber heat absorber the temperature differences are slightly smaller than that of aluminum heat absorber. Aluminium is obviously more effective compared with black rubber as a heat absorber in the distillation unit. A polynomial mathematical model was derived giving predictions that are very close to experimental data with  $R^2$  almost equaled to 1. A result from this experiment is an important step for preparation of full-scale prototype of water distillation unit for rural communities in Thailand.

#### 5. Acknowledgements

The authors gratefully acknowledge the support of the department of Mechanical Engineering, the faculty of Engineering, Khon Kaen University and Thammasat University who provided facilities in this study. The assistance and financial support from the Energy Management and Conservation Office (EMCO) are highly appreciated. This research would also like to thank Kriengkrai Nabudda's research group for assisting with the experiment and data collections.

## 6. References

- [1] Reddy KS, Sharon H, Krithika D, Philip L. Performance, water quality and enviro-economic investigations on solar distillation treatment of reverse osmosis reject and sewage water. *Sol Energy*. 2018;173:160–172.
- [2] Xu Y, Ma J, Liu D, Xu H, Cui F, Wang W. Origami system for efficient solar driven distillation in emergency water supply. *Chem Eng J*. 2019;356:869–876.
- [3] Klungboonkrong V, Phoungchandang S. Microwave drying characteristics and qualities of dried *Orthosiphon aristatus* leaves. *Asia-Pacific J Sci Tech*. 2018;23:1–12.
- [4] Santosh R, Arunkumar T, Velraj R, Kumaresan G. Technological advancements in solar energy driven humidification-dehumidification desalination systems - A review. *J Clean Prod*. 2019;207:826–845.
- [5] Giwa A, Akther N, Housani AA, Haris S, Hasan SW. Recent advances in humidification dehumidification (HDH) desalination processes: Improved designs and productivity. *Renew Sus Energy Rev*. 2016;57:929–944.
- [6] Jayakody H, Al-Dadah R, Mahmoud S. Computational fluid dynamics investigation on indirect contact freeze desalination. *Desalination*. 2017;420:21–33.
- [7] Kaushal AK, Mittal MK, Gangacharyulu D. Development and experimental study of an improved basin type vertical single distillation cell solar still. *Desalination*. 2016;398:121–132.
- [8] Rajaseenivasan T, Elango T, Kalidasa MK. Comparative study of double basin and single basin solar stills. *Desalination*. 2013;309:27–31.
- [9] Al-Nimr MdA, Qananba KS. A solar hybrid system for power generation and water distillation. A solar hybrid system for power generation and water distillation. *Sol Energy*. 2018;171:92–105.
- [10] Zhu Z, Zheng H, Wang Q, Chen M, Li Z, Zhang B. The study of a novel light concentration and direct heating solar distillation device embedded underground. *Desalination*. 2018;447:102–119.
- [11] An W, Chen L, Liu T, Qin Y. Enhanced solar distillation by nanofluid-based spectral splitting PV/T technique: Preliminary experiment. *Sol Energy*. 2018;176:146–156.
- [12] Zhang Y, Liu L, Li K, Hou D, Wang J. Enhancement of energy utilization using nanofluid in solar powered membrane distillation. *Chemosphere*. 2018;212:554–562.
- [13] Phoungchandang S, Suwannasorn W. Computer model for heat transfer Pasteurization of milk using plate heat exchangers. *KKU Res J*. 2008;13:561–567.
- [14] Chen W, Zou C, Li X, Li L. Experimental investigation of SiC nanofluids for solar distillation system: Stability, optical properties and thermal conductivity with saline water-based fluid. *Int J Heat Mass Transf*. 2017;107:264–270.
- [15] Ming X, Guo A, Wang G, Wang X. Two-dimensional defective tungsten oxide nanosheets as high performance photo-absorbers for efficient solar steam generation. *Sol Energy Mater Sol Cells*. 2018;185:333–341.
- [16] Xu J, Xu F, Qian M, Li Z, Sun P, Hong Z, et al. Copper nanodot-embedded graphene urchins of nearly full-spectrum solar absorption and extraordinary solar desalination. *Nano Energy*. 2018;53:425–431.
- [17] Jumrongkut A. *Renewable Energy OS Printing House*. 2002.
- [18] Çengel YA. *Thermodynamics: an engineering approach: Sixth edition*. Boston: McGraw-Hill Higher Education.; 2008.
- [19] Gugulothu R, Somanchi NS, Devendar G, Deepika PKN. Solar water distillation using different phase change materials. *Mater Today: Proceedings*. 2017;4(2, Part A):314–321.
- [20] Sharshir SW, Ellakany YM, Algazzar AM, Elsheikh AH, Elkadeem MR, Edreis EMA, et al. A mini- review of techniques used to improve the tubular solar still performance for solar water desalination. *Process Saf Environ Prot*. 2019;124:204–212.
- [21] Rassamakin B, Khairnasov S, Zaripov V, Rassamakin A, Alforova O. Aluminum heat pipes applied in solar collectors. *Sol Energy*. 2013;94:145–154.
- [22] Ajani C, Curcio S, Dejchanchaiwong R, Tekasakul P. Influence of shrinkage during natural rubber sheet drying: Numerical modeling of heat and mass transfer. *Appl Therm Engine*. 2019;149:798–806.
- [23] Hasanah RN, Indyanto FR, Maulana E, Suyono H. Solar energy hybrid system for seawater distillation in the coastal regions. *Energy Procedia*. 2017;143:662–667.
- [24] Rahbar N, Esfahani JA. Experimental study of a novel portable solar still by utilizing the heat pipe and thermoelectric module. *Desalination*. 2012;284:55–61.
- [25] Kiwan S, Al-Nimr Md, Abdel Salam QI. Solar chimney power-water distillation plant (SCPWDP). *Desalination*. 2018;445:105–114.